Solid Freeform Fabrication 2018: Proceedings of the 29th Annual International Solid Freeform Fabrication Symposium – An Additive Manufacturing Conference
Reviewed Paper

A Novel Microstructure Simulation Model for Direct Energy Deposition Process

Jinghao Li[1], Zhibo Luo[1], Xiaoyi Guan[1], Xianglin Zhou[2], Mathieu Brochu[3], Yaoyao Fiona Zhao[1]*

[1]Department of Mechanical Engineering, McGill University, Montreal, Quebec, Canada H2A0C3
[2]State Key Laboratory for Advance Metals and Materials, University of Science and Technology, Beijing, China 10083
[3]Department of Mining and Materials Engineering, McGill University, Montreal, Quebec, Canada H3A0C5

Abstract

The microstructure of additive manufacturing parts has unique characteristics. In this paper, a novel microstructure simulation model is proposed in grain level, called "Invasion Model", to simulate the transient competitive grain growth behaviour in direct energy deposition (DED) process. Different from the phase field method, the invasion model does not focus on the exact dendrite geometry immersed in the liquid phase which will usually lead into high computational cost. The key point of the invasion model is its capability to reflect the transient competitive grain growth behavior under the triensent thermal gradient located at the bottom of the melt pool. An 'invasion factor' is proposed to represent the possibility that one single crystal will invade its adjacent crystals in each time step. This 'invasion factor' is calculated by the relation between crystallographic orientation and a changing thermal gradient under the help of the grain boundary criterions in competitive grain growth. Furthermore, the shape and the cooling condition of the melt pool are vital to the final microstructure. The geometry of the melt pool is extracted from the temperature history data of finite element and CFD simulation. The melt pool geometry is analyzed quantitively from interpolated temperature history data and inputted into the invasion model. A vertical cross section of DED fabricated Ti-6Al-4V in multiple layers was investigated by the invasion model, and the competitive grain growth behavior is simulated between the crystals with random crystallographic orientations.

1 Introduction and Background

Metal Additive Manufacturing (MAM) methods based on powder, wire, slice metal or alloys are famous for their flexibility, efficiency, and accuracy. They are now changing the landscapes of current industrial practices [1, 2]. However, uncertainties in MAM fabricated parts from microstructure, texture and mechanical properties are restricting its development and application [3]. Different from casting and welding, MAM deposition processes are characterized by heterogeneous nucleation, epitaxial grain

growth and rapid, directional solidification due to the layer by layer build-up fashion. Take DED processed Ti-6Al-4V as an example, some unique microstructural characteristics are shown in Figure 1. The columnar grains are frequently observed to elongate along built direction [4-12], approximately parallel to the preferentially growing directions of prior β grain (shown in Figure 1.a) which is the result of the solidification process that starts at 1660°C. It involves the solidification process of the fusion transfer into crystallographic ordered state phase characterized by body-centered cubic (bcc) crystal structure. The substrate or the previous layer of deposited material acts as a preferential nucleation position on which epitaxial growth starts. Usually, an epitaxially orientated type of growth will develop at the partially melted grains from the substrate. The newly formed grains will inherit crystallographic effects such as existing grain orientations from existing crystals. Due to the heat accumulation process during the additive manufacturing, the material in different layers will go through different temperature history resulting in different solid phase composition. Various solid phase composition conditions along with the newly added deposition layers are depicted as position-dependent microstructural "maps" (Figure 1.b) based on known relationships among the thermal history and microstructural evolution. The microstructural and mechanical properties of the deposited material depend strongly on the thermomechanical cycle. Melt pool models in welding have been used as a guide for MAM process and microstructure simulation. However, existing thermal welding models were found to be inadequate for describing the MAM process due to inconsistencies in predictions of the microstructures [13-15].

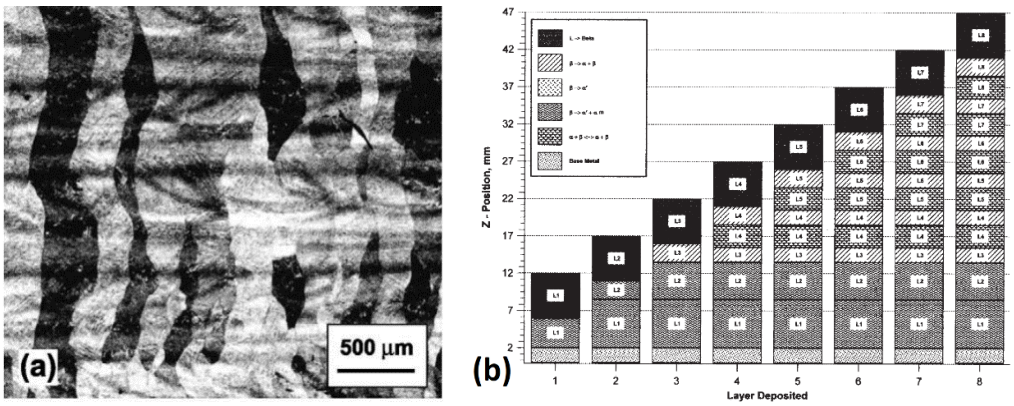

(a) Column grains and Epitaxial growth (b) Microstructural evolution map of the build as each layer is deposited

Figure 1. Microstructural characteristics in Ti-6Al-4V fabricated by Direct Energy Deposition [16, 17]

Study on dendritic growth and features of the crystal grain is a prominent fundamental research topic in microstructure modelling and simulation. In the current solidification microstructure simulation research, physical models act as the foundation providing formal description of the crystal nucleation and grain growth behavior. Microstructural factors such as grain size and texture are calculated under different algorithms through the numerical simulation and implemented on computer visualization. Currently, there

are four methods widely used in the field of microstructure simulation in grain scale, namely cellular automata, phase field, Monte Carlo and deterministic approaches. The deterministic methods are based on solidification kinetics, usually with clear application background. However, due to its oversimplification and neglection of stochastic factors, it can rarely reflect the solidification phenomenon such as nucleation orientation and competitive grain growth. Cellular automata method is suitable for MAM microstructure simulation with relatively low computational cost. It is also able to provide the information on grain outline in multiple layers [18-20]. Compared to analytical models, cellular automata offers the additional advantage of providing a direct view of the grain structure and texture [21]. However, the essence of cellular automata method is based on the local or short term rules. The neighborhood strategy, cell scale inevitably effect the simulation result even for a simple bi-crystalline system [22]. Even though the phase field method is strictly based on physical model and able to offer a high reproduction of the reality, it can only generate one or a few grains in the simulation process with massive computation demand. When phase field is carried out on the 3D level, the situation of computational expensive becomes unacceptable. As for Monte Carlo method, it is simple and effective in simulating grain growth behavior especially the recrystallization, but it can only provide the result of final stage from large numbers of ‘trials and error'. Recently, researhcers are also working on the kinetic Monte Carlo method to carry out microstructure simulation between the time steps of thermal field simulations [23, 24].

MAM parts are composed of a large number of welds. The microstructures of AM components depend strongly on cooling condition of the melt pool and the solid phase transformation in a single weld. Thus, the melt pool shape is the direct reflection of the cooling condition of the weld and vital to the final grain texture. On the other hand, part geometry will undoubtedly affect the cooling condition of the melt pool. Thus, a part-level microstructure simulation model is needed to analyze the part geometry effect on the MAM microstructure. In the reviewed published works, the shape of the real-time melt pool and the transient thermal gradient direction are usually simplified or even ignored: For phase field method, the simulations are mostly carried out on a small research area under the frozen temperature gradient approximation with constant thermal gradient direction [25-27]. In Monte Carlo method, even though the simulation area is located near the melt pool bottom, it does not consider the transient thermal gradient at each point and currently does not incorporate material texture or anisotropy [23, 24]. The CA method is able to take the exact melt pool geometry in to account [20], however due to the mentioned essential defects [28], new methods should be developed.

In this work, an invasion model is proposed based on the accurate reproduction of the melt pool geometry. The competitive grain growth behavior will be described in section 2.2.2. An ‘invasion factor' which means the opportunity that one single crystal can invade its adjacent crystals in a single time step is introduced in section 2.2.3. This ‘invasion factor' is calculated by the relation between crystallographic orientation and a changing thermal gradient along the entire area of melt pool bottom under the help of

the grain boundary criterions. The solidification process including the nucleation and grain growth will be detailly described in the following sections. In this work, DED fabricated Ti-6Al-4V is selected as a simulation target, and the primary β dendritic column grains in Ti-6Al-4V are called ‘grains' or ‘column grains' for the sake of simplicity.

2 Numerical Modelling

The overall modelling roadmap of the invasion model’s implementation in DED process is shown in Figure 2. Based on the temperature history provided by the finite element (FE) and melt pool computational fluid dynamics (CFD) simulation, the temperature data is interpolated to match with 5μm square cells. The temperature history data is provide by the co-authors from their previous [29] and unpublished work. The data is preprocessed to locate the melt pool position and accurately depict the geometry of the melt pool referring to the solidus line. The rescaled temperature history data together with the melt pool information is the input into invasion model. Prior to this step, the material properties, part geometry, scanning strategy and substrate crystallographic orientation will be preprocessed into the model as boundary conditions. If the simulation results are independent of the discretization issues in time and space, the experimental validation will be used to improve the accuracy of the model. Reconstructed electron backscattered diffraction (EBSD) and grain size statistics are ideal aspects to compare with the simulation result. However, for Ti-6Al-4V alloy, the solid phase transformation usually eliminates most of the crystallographic orientation information of the β grains. So, the β type alloy will be an optional choice for the validation of the model. The grain geometry, crystallographic orientation and grain size will be the output of the invasion model. However, these are inadequate to predict the mechanical properties of the final part. The solid phase prediction model developed by Kelly and Kampe [17] was employed in this simulation procedure. The solid phase compositions are depicted as a microstructural evolution map of the build as each layer is deposited. In this section, several concepts will be introduced and the algorithm for the invasion model will be described in detail.

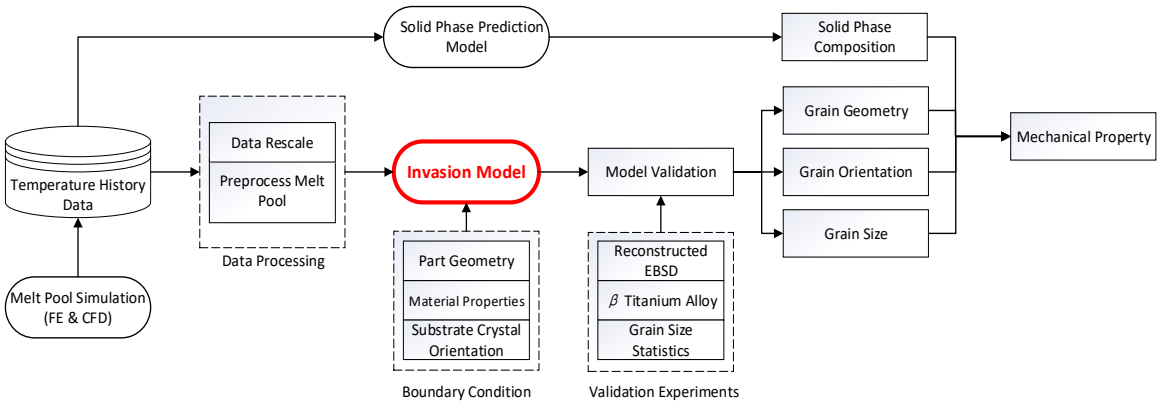

Figure 2: Flowchart of the microstructure simulation for Ti-6Al-4V in AM

2.1 Nucleation Theory

Nucleation is the first step of solidification process. In the deterministic models of solidification, the heterogeneous nucleation theory is widely used to explain the small undercooling needed for a conventional solidification process. However, in the heterogeneous nucleation theory, if the nuclei simultaneously generate at a critical undercooling value, it is not able to explain the grain density changes in different cooling conditions. This is contrary to observation, where the grain size will decrease dramatically in a higher cooling rate. Now, the instantaneous nucleation theory is broadly accepted by the researchers and implemented into microstructure simulation. This theory believes the nucleation phenomenon is a thermal-activated process and the grain density increase is a function of supercooling

$$\frac{dn}{d(\Delta T)} = \frac{n_{max}}{\Delta T_\sigma \sqrt{2\pi}} \frac{1}{\Delta T} \exp\left[-\frac{1}{2}\left(\frac{ln\Delta T - ln\Delta T_0}{\Delta T_\sigma}\right)^2\right] \quad (1)$$

where the number of newly formed nuclei per unit volume dn between ΔT and $\Delta T + d(\Delta T)$ is illustrated by a Gaussian distribution. n_{max} is the total density of nucleus positions, ΔT_σ is the standard deviation, and ΔT_0 is the mean value of the supercooling distribution.

In the aspect of nucleation behavior in MAM, the epitaxial growth is a common phenomenon, and a single crystal can run through multiple layers of material deposition in DED Ti-6Al-4V samples [11]. In some cases, the column grains even grow throughout the entire length of the printed part. If we consider the previously formed layer as the substrate to heterogeneous nucleation, there will be perfect compatibility between these two phases. Theoretically, there is no nucleation energy barrier, and the wetting angle is zero. It means there is no or little newly formed nuclei in the material deposition process. Thus, the instantaneous nucleation will be neglected in the case of the invasion model presented in this work. The column grains will directly epitaxially grow from a crystallographic orientation and grain geometry defined substrate. These boundary conditions of crystallographic orientation should be measured by experiments.

However, the external factors such as impurity and unmelt metal powders are the main reason for new nuclei in MAM. Take selective laser melting (SLM) as an example, the layer thickness is so small (20-50 μm) which needs more powder shaving processes. Also, the small laser power and laser beam diameter in SLM leads to small melt pool which will result in unmelt powders. These aspects leave more opportunities for the external factors intervention and nucleation behavior cannot be neglected, and the instantaneous nucleation behavior (equation-1) should be applied.

2.2 The Proposed Invasion Model

Different from the physical based cellular automata methods representing the grain growth by dendrite tip growth kinetics, the invasion model is looking for a method to describe the interactions between the adjacent grains during the solidification. An

invasion factor will be introduced to analyze the competitive grain growth behavior quantitively. The mushy zone where the competitive grain growth happens is assumed to be extremely small. It is located at the bottom of the melt pool and in the numerical simulation, represented by a curved slice of cells. By introducing the invasion model, the long-term relations of grain boundary will be represented locally and on a small scale. The changing of supercooling between the neighboring cells will be neglected in the case of invasion model which is presented here.

2.2.1 Dendrite growth orientation

In DED fabricated samples, the prior-β column grains are frequently observed to elongate along the build direction with a <100>$_\beta$ fiber texture. The reason is the cubic crystal systems have preferred growth directions in the direction of <100> crystallographic orientation. This phenomenon was first conducted by Walton and Chalmers [30], they summarized that the grains with preferred growth direction aligned with temperature gradient could get a more significant opportunity to win the competitive grain growth. The details in competitive grain growth and grain boundaries will be discussed in the next section.

In the aspect of crystallography, the point group of cubic system is described as P 4/m $\bar{3}$ 2/m (m3m). It means that the axis in <100> directions is a 4-fold symmetry. If we consider a two-dimensional simulation system, the crystallographic orientation can only change from -π/4 to +π/4 referring to the temperature gradient direction.

2.2.2 Grain boundary algorithm for growth competition

There are two criterions to describe the interaction between the adjacent crystals in the competitive grain growth, called Geometrical Limit (GL) and Favorably Orientated Grain (FOG) criterion, respectively. The GL criterion considers every dendrite is containing infinitely small branches with growth directions perpendicular to their main dendrite arms. The FOG criterion is a simple idea that the grains having the growth direction best aligned with the temperature gradient will survive the competitive grain growth. Take GL criterion as an example, if we consider the (a)diverging and (b)converging primary dendrite trunks as shown in Figure 3. The relations between temperature gradient and crystallographic orientation can be expressed as (detailed derivation can be found in [22]):

$$\theta_{GL}(\alpha_1,\alpha_2)\begin{cases}\tan^{-1}\left(\frac{\cos\alpha_1+\sin\alpha_1-\sec\alpha_2}{\cos\alpha_1-\sin\alpha_1}\right) & if\ (\alpha_1+\alpha_2)\geq 0\ and\ (\alpha_1<\alpha_2)\\ \tan^{-1}\left(\frac{\sin\alpha_2-\cos\alpha_2+\sec\alpha_1}{\cos\alpha_2+\sin\alpha_2}\right) & if\ (\alpha_1+\alpha_2)<0\ and\ (\alpha_1<\alpha_2)\\ \left(\frac{\alpha_1+\alpha_2}{2}\right) & if\ (\alpha_1>\alpha_2)\end{cases} \quad (2)$$

where the orientation angles for the primary trunks of the left-hand-side grain is α_1, and the right-hand-side grain is α_2, the resultant grain boundary angle θ.

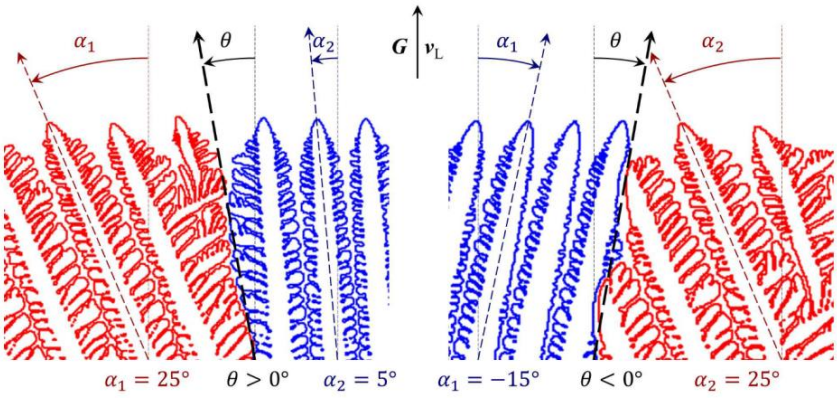

Figure 3. Competitive grain growth at the grain boundary of a bi-crystal [22]

2.2.3 Invasion factor

An invasion factor is a dimensionless number used in calculations involving competitive grain growth behavior. It is the arctangent value of the grain boundary inclination angle (θ_{GB}) under the absolute coordinate system, for example, the printing coordinate in MAM. As discussed in section 2.2.1, the crystallographic orientation, α_1 and α_2, can only change from -π/4 to +π/4 referring to the temperature gradient direction. Thus the $\theta_{GL}(\alpha_1, \alpha_2)$ is also with an absolute value under π/4, and the invasion factor in the locally thermal gradient coordinate is a value under one. It represents the opportunity one cell can occupy its adjacent GB cell, and only the cells with higher invasion factor value can invade those with small. However, if we transfer the time and space dependent temperature gradient coordinate into the absolute coordinate, the invasion factor can be higher than one. Then the invasion factor means how many cells can be occupied in a single time step. In each time step, there is only one slice of cells can be activated, and theoretically the θ_{GB} will be constant under different cell magnitude.

2.2.4 Implementation of simulation

In the invasion model, a regular mesh of square cells of the same size discretizes the computational domain. The Moore configuration is used to define the neighborhood，and the temperature history will be provided by macroscale simulations at a part or melt-pool level and will be matched with grids of invasion model by a differential algorithm. As shown in Figure 4, a moving window will follow the melt pool region and divide the cells into fusion cell, mushy cell and solid cell respectively. The grain boundary cell (GB cell) will be found among the mushy cells. These GB cells are also the locations where invasion factor becomes valid and competitive grain growth take place. The crystallographic orientation information of solid cells belonging to different crystals will be stored and visualized by the invasion model.

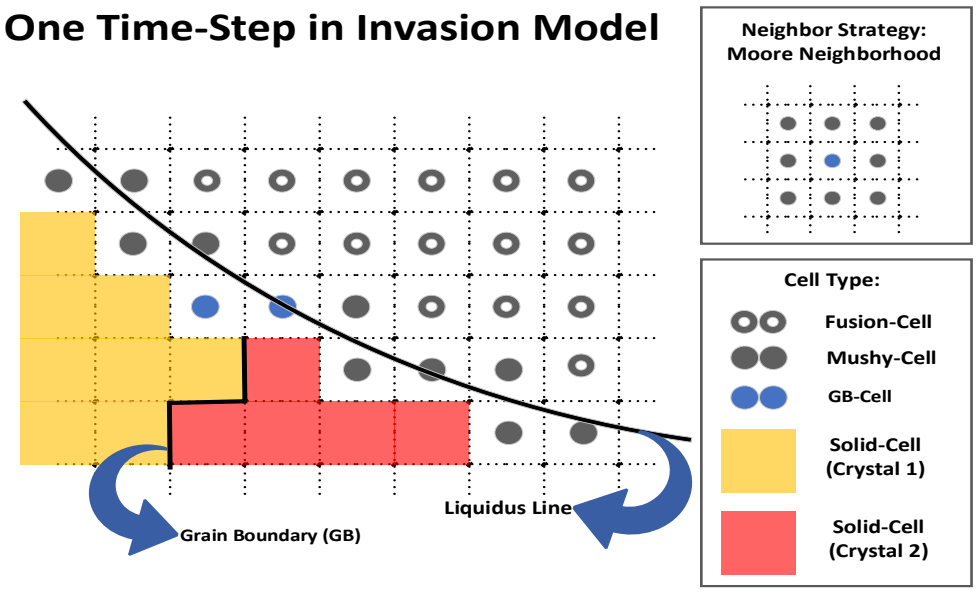

Figure 4. Schematic of the cell type definition in the invasion model

Following the workflow chart shown in Figure 5, the invasion model should include the following steps:

(1) Substrate microstructure simulation: this step can be achieved by a 2D microstructure simulation or the experiment data including the information of microstructure patterns and orientation of the substrate material. At the first stage, it can also be simplified as equiaxial grains with random orientations.

(2) Object region activated and partition: transient temperature field will be loaded at the object region (representing the materials added region of DED) and divided into three areas, namely solid, mushy zone and fusion zone.

(3) Identify the grain growth area and start point: The crystallographic orientation of the grains will generate between the solidus surface in two time-steps of macro-scale simulation. The start positions are the cells located along the solidus line without crystallographic orientation (mushy cells).

(4) Epitaxial growth and grain boundary invasion: A similar cellular automata algorithm will come into effect in this step, and here we only consider a 2D neighbor strategy with eight neighbors as an example. The cellular along the solidus surface without crystallographic orientation will be assigned orientation based on the following rules:

   a. If a cellular has neighbors with same crystal orientation, it will inherit the orientation directly from the bottom layer

   b. If a cellular has neighbors with different crystallographic orientation (located near grain boundaries), the invasion factor of these neighbors will be compared, and the mushy cells will have the most significant possibility to inherit the orientation factors of the neighboring cells with highest invasion factor.

(5) Continuous simulation: Jump to the start point identification in step 3 when all the mushy-cells are assigned with crystallographic orientation and find another layer of

mushy-cell. If all the solid phase regions have been assigned crystallographic orientation factor, jump to the next time step of macroscale simulation temperature field data.

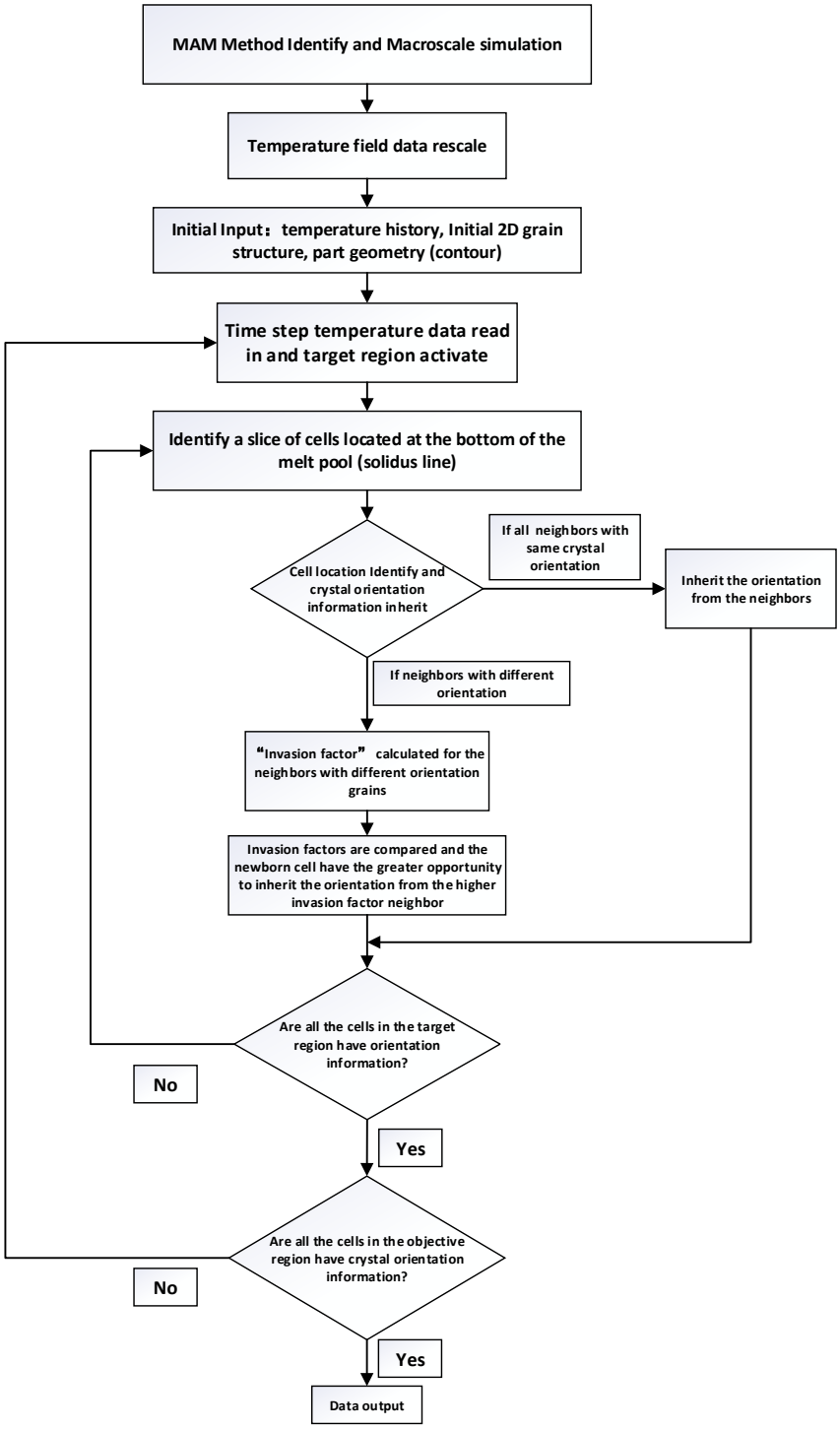

Figure 5. Flowchart of the invasion model

2.3 Model Validation Methods

This work only provide the morphology of the novel microstructure simulation method. In the further publish work, the model will be validated in the following three aspects:

(1) When the temperature of DED fabricated Ti-6Al-4V parts is decreased to its β-α transus line, the prior β phase will transfer to α phase. In the view of crystallography, the bcc (body center cubic) lattice structure into an hcp (hexagonal closed-packed) order, following the Burgers orientation relationship (BOR):

$$\{110\}\beta_{bcc} \parallel \{0002\}\alpha_{hcp} \,\&< 111 > \beta_{bcc} \parallel < 11\bar{2}0 > \alpha_{hcp}$$

EBSD has provided a quantitative tool to study microstructures in large scales. Following the BOR mentioned above, the hcp phase which pre-transformed at β-α transus temperature can be reconstructed into the bcc order (prior β phase). The grain boundary of prior β phase can be depicted with each grain crystallographic orientation represented quantitively. It is a good way to validate the microstructure simulation model in grain size. Moreover, in most of the research work in the literature, the substrate is set up with equiaxed grains with random crystallographic orientation. To make the simulation result more accurate and closed to reality, the reconstructed EBSD result on the substrate section can be used as the boundary conditions of the simulation model.

(2) The β type titanium alloys can also be used as target alloy to avoid the solid phase transformation. Because the prior β phase of β type titanium alloys can be kept until the room temperature, it is relatively closed to the prior generated grains when the liquid phase first transfer into a crystallographic ordered bcc structure.

(3) The primary target of the invasion model is to compute the competitive grain growth behavior quantitively under time and space dependent temperature gradient, and the invasion behavior will result in a changing grain size along the building direction. Thus, the grain size statistics is a simple and efficient way to compare the simulation output with the experimental result.

3. Simulation Result

3.1 The Geometry of Melt Pool and Transient Thermal Gradient

The shape of melt-pool is generated at each discrete time step according to the temperature history data. The shape of the melt pool plays a vital role in the MAM microstructure; it is a direct reflection of the transient process parameters and the cooling condition. Before the temperature history data is input into the invasion model, the melt pool geometry will be analyzed quantitively in the aspects of width, depth, length and compared with double-ellipsoid melt pool model [31, 32]. Also, the cooling state of the melt-pool including time and space dependent temperature gradient along the melt pool bottom will be calculated based on the temperature history data.

As shown in Figure 6, the transient geometry of melt pool is extracted from the temperature history in two timesteps of the FE simulation results (green for the first timestep and red for the second). The crystal information will be eliminated in the re-melt area of the substrate or previous layer. The gap between the tails of melt pool is the target area for invasion model to generate the new crystal following the movement of the melt-pool (shown in Figure 4). Between the two timesteps of the macroscale simulation result, the invasion model divides the area of melt-pool tails into multiple sub-timesteps based on the magnitude of the cells. In each fleeting moment, the invasion factor of the GB cells will be calculated based on the cells' transient thermal gradient and crystallographic orientation.

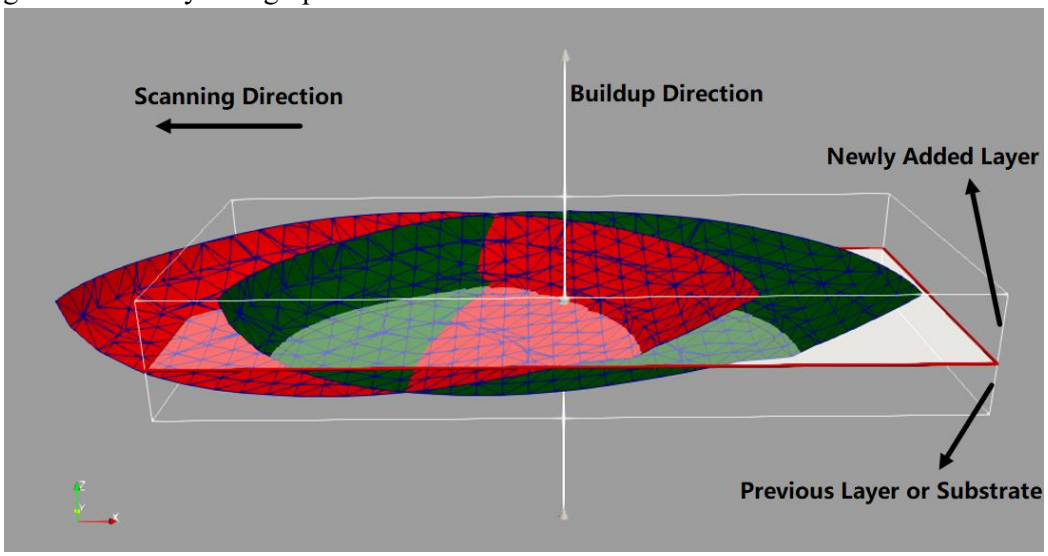

Figure 6. The shape of melt-pool in two timesteps of the macroscale model

3.2 Multiple Layer Deposition and Competitive Grain Growth

Simulated microstructures using a unidirectional scanning strategy in multiple layers of material deposition in DED Ti-6Al-4V is investigated by the invasion model, shown in Figure 7.

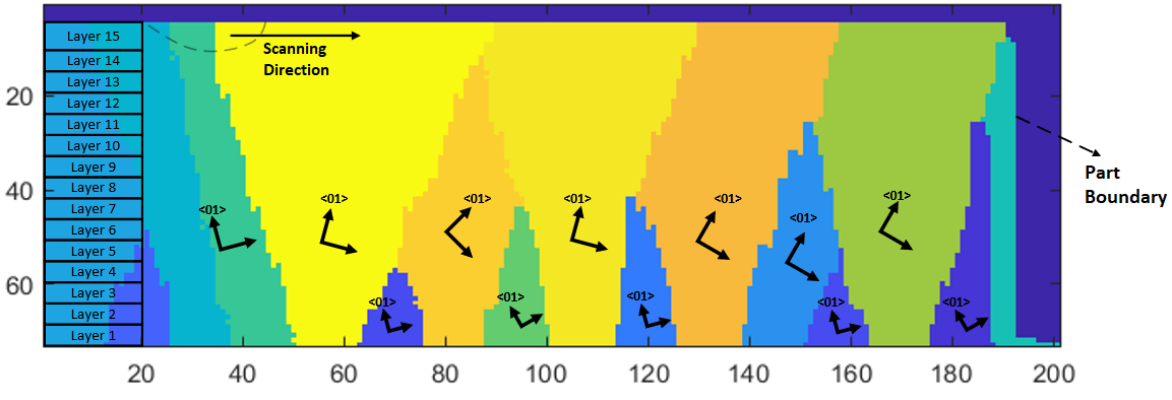

Figure 7. The competitive grain growth in the invasion model

By extracting the temperature history data of previous 3D finite element simulation at the vertical cross-section (symmetry plane) of a thin wall structure, the 2D invasion model simulation is applied to depict the competitive grain growth behavior. For the case shown above, the program coding is under C++ and Matlab, and the simulation takes 25 minutes under a single CPU (i7-8086K processor) including the data preprocessing and interpolation time. The crystallographic orientation is given randomly at the bottom layer, and the part boundary is also settled as the boundary condition. From the simulation result, the crystals with crystallographic orientations best aligned with the temperature gradient get a chance for grain growth, even with enormous resultant grain size. On the other hand, the crystals with unfavored orientations will be swept out after a few layers of deposition. Note that, the solid and liquid interface of every single crystal in DED process is facing a time-dependent temperature gradient. The changing thermal gradient direction will result in a curvature grain geometry along the grain growth direction. However, because of the rapid solidification rate of the melt pool and the remelting of the previous layer, this phenomenon is not obvious on the present simulation result.

4. Conclusions

This paper proposes an invasion model, which consists of grain crystallographic orientation and the transient thermal gradient, to simulate the microstructure of the DED fabricated Ti-6Al-4V part. The invasion model is more efficient in tracking the geometry of grain boundaries on a large scale. Besides the dendrite tip growth kinetics, the invasion model takes advantages of the grain boundary criterions and reflect the competitive grain growth behavior quantitively. Base on the accurate analysis of the real-time melt pool geometry, the microstructure and texture in multiple layers of DED processed Ti-6Al-4V thin wall structure is simulated by the invasion model. The change of the grain size will be compared with experimental result in the further development of this model. For now the model is only a preliminary version, continuous work of this research also includes the investigation of the influence of the part geometry and scanning strategy, as well as the implement in a 3D part-level microstructure simulation.

Acknowledgements

This research work is supported by AMOS Project (NSERC and CARIC CRDPJ 479630-15), the National Key Research and Development Program of China (Grant No. 2018YFB0703400) and China Scholarship Council (201706460027).

5. Reference

1. Chua, C.K. and K.F. Leong, *3D Printing and Additive Manufacturing: Principles and Applications (with Companion Media Pack) of Rapid Prototyping Fourth Edition*. 2014: World Scientific Publishing Company.

2. Gao, W., et al., *The status, challenges, and future of additive manufacturing in engineering.* Computer-Aided Design, 2015. **69**: p. 65-89.
3. Greitemeier, D., et al., *Uncertainty of Additive Manufactured Ti-6Al-4V: Chemistry, Microstructure and Mechanical Properties.* Applied Mechanics and Materials, 2015. **807**: p. 169-180.
4. Sames, W.J., et al., *The metallurgy and processing science of metal additive manufacturing.* International Materials Reviews, 2016. **61**(5): p. 315-360.
5. Raghavan, N., et al., *Numerical modeling of heat-transfer and the influence of process parameters on tailoring the grain morphology of IN718 in electron beam additive manufacturing.* Acta Materialia, 2016. **112**: p. 303-314.
6. Lin, J.J., et al., *Microstructural evolution and mechanical properties of Ti-6Al-4V wall deposited by pulsed plasma arc additive manufacturing.* Materials & Design, 2016. **102**: p. 30-40.
7. Herzog, D., et al., *Additive manufacturing of metals.* Acta Materialia, 2016. **117**: p. 371-392.
8. Frazier, W.E., *Metal Additive Manufacturing: A Review.* Journal of Materials Engineering and Performance, 2014. **23**(6): p. 1917-1928.
9. Wang, F., et al., *Microstructure and Mechanical Properties of Wire and Arc Additive Manufactured Ti-6Al-4V.* Metallurgical and Materials Transactions A, 2012. **44**(2): p. 968-977.
10. Wang, F., S. Williams, and M. Rush, *Morphology investigation on direct current pulsed gas tungsten arc welded additive layer manufactured Ti6Al4V alloy.* The International Journal of Advanced Manufacturing Technology, 2011. **57**(5-8): p. 597-603.
11. Kobryn, P. and S. Semiatin, *The laser additive manufacture of Ti-6Al-4V.* Jom, 2001. **53**(9): p. 40-42.
12. Thijs, L., et al., *A study of the microstructural evolution during selective laser melting of Ti–6Al–4V.* Acta Materialia, 2010. **58**(9): p. 3303-3312.
13. Semak, V.V., *Melt pool dynamics during laser welding.* J. Phys. D: Appl. Phys, 1995. **28**: p. 2443.
14. Karimzadeh, F., A. Ebnonnasir, and A. Foroughi, *Artificial neural network modeling for evaluating of epitaxial growth of Ti6Al4V weldment.* Materials Science and Engineering: A, 2006. **432**(1-2): p. 184-190.
15. David, S., S. Babu, and J. Vitek, *Welding: Solidification and microstructure.* Jom, 2003. **55**(6): p. 14-20.
16. Kobryn, P.A. and S.L. Semiatin, *Microstructure and texture evolution during solidification processing of Ti–6Al–4V.* Journal of Materials Processing Technology, 2003. **135**(2-3): p. 330-339.
17. KAMPE, S.M.K.a.S.L., *Microstructural Evolution in Laser-Deposited Multilayer Ti-6Al-4V Builds.* METALLURGICAL AND MATERIALS TRANSACTIONS A, 2004.
18. Zhang, J., et al., *A coupled finite element cellular automaton model to predict thermal history and grain morphology of Ti-6Al-4V during direct metal deposition (DMD).* Additive Manufacturing, 2016. **11**: p. 32-39.

19. Rai, A., M. Markl, and C. Körner, *A coupled Cellular Automaton–Lattice Boltzmann model for grain structure simulation during additive manufacturing.* Computational Materials Science, 2016. **124**: p. 37-48.
20. Zinoviev, A., et al., *Evolution of grain structure during laser additive manufacturing. Simulation by a cellular automata method.* Materials & Design, 2016. **106**: p. 321-329.
21. Rappaz, M., *Modeling and characterization of grain structures and defects in solidification.* Current Opinion in Solid State and Materials Science, 2016. **20**(1): p. 37-45.
22. Pineau, A., et al., *Growth competition between columnar dendritic grains–Cellular Automaton versus Phase Field modeling.* Acta Materialia, 2018.
23. Rodgers, T.M., J.D. Madison, and V. Tikare, *Simulation of metal additive manufacturing microstructures using kinetic Monte Carlo.* Computational Materials Science, 2017. **135**: p. 78-89.
24. Popova, E., et al., *Process-structure linkages using a data science approach: application to simulated additive manufacturing data.* Integrating Materials and Manufacturing Innovation, 2017. **6**(1): p. 54-68.
25. Keller, T., et al., *Application of finite element, phase-field, and CALPHAD-based methods to additive manufacturing of Ni-based superalloys.* Acta materialia, 2017. **139**: p. 244-253.
26. Gong, X. and K. Chou, *Phase-Field Modeling of Microstructure Evolution in Electron Beam Additive Manufacturing.* Jom, 2015. **67**(5): p. 1176-1182.
27. Sahoo, S. and K. Chou, *Phase-field simulation of microstructure evolution of Ti–6Al–4V in electron beam additive manufacturing process.* Additive Manufacturing, 2016. **9**: p. 14-24.
28. Wolfram, S., *Computation theory of cellular automata.* Communications in mathematical physics, 1984. **96**(1): p. 15-57.
29. Luo, Z. and Y.F. Zhao, *Numerical simulation of temperature fields in powder bed fusion process by using hybrid heat source model.* Solid Freeform Fabrication 2017: Proceedings of the 28th Annual International 2017.
30. Walton, D. and u.B. Chalmers, *The origin of the preferred orientation in the columnar zone of ingots.* Transactions of the American Institute of Mining and Metallurgical Engineers, 1959. **215**(3): p. 447-457.
31. Goldak, J., A. Chakravarti, and M. Bibby, *A new finite element model for welding heat sources.* Metallurgical transactions B, 1984. **15**(2): p. 299-305.
32. Liu, W. and J. DuPont, *Effects of melt-pool geometry on crystal growth and microstructure development in laser surface-melted superalloy single crystals: Mathematical modeling of single-crystal growth in a melt pool (part I).* Acta materialia, 2004. **52**(16): p. 4833-4847.